Advances in Colloid and Interface Science 168 (2011) 93–104

Contents lists available at ScienceDirect

Advances in Colloid and Interface Science

journal homepage: www.elsevier.com/locate/cis

Hofmeister effect on micellization, thin films and emulsion stability

Ivan B. Ivanov [a,*], Radomir I. Slavchov [b], Elka S. Basheva [a], Doroteya Sidzhakova [a], Stoyan I. Karakashev [b]

[a] Laboratory of Chemical Physics & Engineering, University of Sofia, 1164 Sofia, Bulgaria
[b] Department of Physical Chemistry, University of Sofia, 1164 Sofia, Bulgaria

ARTICLE INFO

Available online 16 June 2011

Keywords:
Ion specific effects
Hofmeister series
Adsorption of ions
CMC of ionic surfactants
Thin liquid films
Film trapping technique

ABSTRACT

The Hofmeister effect on the critical micelle concentration (CMC), the thin liquid film electrostatic disjoining pressure (Π_{el}) and the critical coalescence pressure of emulsion drops (P^{CR}) were investigated. For CMC literature data were used, but Π and P^{CR} were measured by us. The essence of the theoretical approach was to modify existing theories of CMC and Π_{el} by using generalized Gouy equation and dimensionless surface potential (Φ^S), involving the counterion specific adsorption energy (u_0). The computational procedure of u_0 does not involve any adjustable parameters. Linear dependences of ln(CMC), Φ^S and P^{CR} on u_0 were found in conformity with Hofmeister series. The experimental slopes of ln(CMC) and Φ^S vs. $-u_0/k_BT$ were negative and very close to the theoretical ones. A hypothesis was put forward for explanation of the positive slopes of P^{CR} on u_0. The obtained results suggest that the counterion specific adsorption energy u_0 encompasses all major factors, involved in the Hofmeister effect for the studied phenomena. If this is confirmed by analysis of more phenomena, revealing Hofmeister effect, one could claim that u_0 is the factor controlling the Hofmeister effect and a powerful tool for its study.

1. Introduction

In 1887 F. Hofmeister published his famous article [1] "About regularities in the protein precipitating effects of salts and the relation of these effects with the physiological behavior of salts" (which is part of a series of seven papers entitled "About the science of the effect of salts"; see also Ref. [2]). It was devoted mainly to the study of the precipitating efficiency of salts on proteins. Hofmeister ordered the ions by efficiency in what is now known as "Hofmeister series". Part of this series, which is related to the present study, is quoted below:

$$\begin{aligned}&\text{Cations}: Li^+ < Na^+ < NH_4^+ < K^+ < Cs^+\\ &\text{Anions}: OH^- < F^- < CH_3COO^- < Cl^- < Br^- < NO_3^- < I^- < ClO_4^-\end{aligned} \quad (1)$$

The Hofmeister effect is related to many phenomena besides the protein solubility. Among them are the surface tension of electrolyte solutions, the electrolyte activity, pH measurements, zeta potentials, buffers, micellar properties and critical micelle concentrations (CMC), micro-emulsion structure and vesicles, enzymatic catalysis, lipid monolayers, polyelectrolytes, nano-crystals, DNA aggregation, etc. In a special issue of *Current Opinion in Colloid and Interface Science* [3] the interested reader can find a collection of papers on most of the subjects mentioned above.

Earlier attempts for interpretation of the Hofmeister series and its effect on the interaction between proteins, macromolecules or colloidal particles were qualitative and invoked mainly the ion size, the ion interaction with water and the "hydration force". The latter was defined by Kunz et al. [4] as "what remains after subtraction of the van der Waals force and the double layer force from the experimentally measured interaction force". Ninham (see Refs. [5–7] and the references therein) was probably the first to advocate the role of the van der Waals forces for the interaction between ions in solution, for the adsorption of electrolytes, for the interaction between proteins or colloidal particles etc. His suggestion, going against the commonly used assumption that these interactions are dominated by the much stronger electrostatic interactions, is based on the argument that even moderate electrolyte concentrations can screen the electrostatic interactions without substantially affecting the van der Waals forces. Moreover, since the van der Waals forces increase steeply with decreasing distance (roughly with the sixth power), they may become if not dominant, at least very important for phenomena, occurring at short distances, such as adsorption of ionic species and micellization.

Following Ninham's ideas, we proposed in Ref. [8] a relatively simple theory of the effect of the type of electrolytes on the adsorption constant of ionic surfactants. In the core of the theory is a quantity, u_0, which we call *ion specific adsorption energy* — it is equal to the van der Waals adsorption energy of an ion at the interface. It turned out to be independent on the type of the surfactant, which allows using the calculated value for a given ion for interpretation of adsorption data for different surfactants and hopefully — to apply it to the interpretation of other related phenomena. The test of the theory

* Corresponding author. Tel.: +359 2 9625310; fax: +359 2 9625643.
E-mail address: ii@lcpe.uni-sofia.bg (I.B. Ivanov).

0001-8686/$ – see front matter © 2011 Elsevier B.V. All rights reserved.
doi:10.1016/j.cis.2011.06.002

against surface tension data for sodium dodecylsulfate, ($C_{12}H_{25}SO_4Na$), with counterions Li^+, Na^+ and K^+, and dodecyltrimethylammonium bromide, ($C_{12}H_{25}NMe_3Br$, where "Me" denotes methyl group), with counterions F^-, Cl^- and Br^- gave very encouraging results. For more details see Ref. [8] and Section 2 below. Recently we extended and improved the theory and confirmed it with several surfactants each with several counterions (paper in preparation).

Our ambition in this article is to subject this theory to another rigorous *quantitative test* by applying it to phenomena, related to Hofmeister effect, but having different nature and mechanism from surfactant adsorption. As new tests we chose interpretation of the data on the effect of the type of electrolyte (**i**) on the value of the critical micelle concentration, (**ii**) on the disjoining pressure of thin liquid films and (**iii**) on the emulsion stability.

We did not find any experimental data (nor theoretical considerations) about the effect of the type of electrolytes on the disjoining pressure and emulsion stability — hence, we performed the experimental studies by ourselves. On the contrary, there are numerous data and attempts for *qualitative* interpretation of the effect of the concentration and type of electrolytes on the critical micelle concentration, CMC (see Section 3 below). The counterions of different salts have been found to follow Hofmeister series. Fair correlations of micellization parameters with hydrated ion radius and lyotropic number of ions have been found to be operative, e.g. Refs. [9,10].

Kunz et al. [4] analyzed some studies of the physico-chemical parameters, taken into consideration to rationalize and order Hofmeister phenomena, such as the lyotropic number, the Gibbs free energy and entropy of hydration of cations and anions, surface tension increment, polarizability, partial molar volume, molar refractivities, entropy change of water, variation of the "empty volume of the solvent". They called them "attempts to order phenomena, in the absence of a definite firmly based theory… because, most probably, there is no ONE factor involved in Hofmeister effects" [4].

In Refs. [7,11] Ninham and associates wanted to "show the undoubted importance of ionic dispersion forces" for interaction between interfaces and micellization. That is why they neglected (but mentioned) some other effects, such as interactions of water with single ions (hydration numbers and radii), different ways of interaction of water with cations and with anions, leading to different interaction of the hydrated ions with the interface etc. [4].

Our theory of the Hofmeister effect accounts in a simplified manner for most of the necessary effects, mentioned by Kunz et al. [4]. Its moderate success in predicting quantitatively the ion specific effects on the adsorption constant of ionic surfactants and the results obtained in the present study make us believe that it is close to a "firmly based theory" whose absence was deplored by Kunz et al. [4]. Moreover, it seems that the ion specific adsorption energy, u_0, introduced in Ref. [8] and used also here, could be considered as the "factor involved in Hofmeister series" [4].

The paper is organized as follows. For reader's convenience in Section 2 a brief account of the theory from Ref. [8] is presented. Section 3 is devoted to the theory and data analysis of CMC. In Section 4 the experimental data about the dependence of the thin film disjoining pressure and their theoretical analysis are presented. We studied the emulsion stability by two different methods, applied to different systems (single drops and bulk emulsion) but leading to the same final result — the critical pressure of film rupture, P^{CR}, controlling the drop coalescence. The respective techniques, Film Trapping Technique (FTT) and Centrifugation, are described along with the data analysis in Section 5. Some more important conclusions are summarized in Section 6.

2. Theory of the specific effects on surfactant adsorption (basic concepts and equations)

In Ref. [8] we developed and checked experimentally a theory of the ion specific effect on the adsorption of surfactants. The basic equations derived there are applicable also to the phenomena studied in the present article and will be used below. To facilitate the reader we give in this Section a brief summary of the basic concepts and equations underlying the treatment below. Details can be found in Ref. [8].

2.1. Combined surface potential

We accounted for the van der Waals interaction energy $u_v(z)$ of the counterions with the liquid phase by the simple equation (obtained by integrating London equation, see e.g. [12]):

$$u_v(z) = u_0 \frac{R^3}{(R+z)^3}, \tag{2}$$

where z is the distance to the interface, R is the ionic radius (of the bare or of the hydrated ion, R_i or R_h respectively) and u_0 is the van der Waals energy when the ion is in the plane $z=0$ (for short we refer to u_0 as *ion specific adsorption energy*). We considered only high enough surface potentials, allowing neglecting (at the final stage of the calculations) the presence of surfactant ions and coions in the diffuse layer and thus accounting only for one van der Waals energy, that of the counterions. Thus, the calculation of the electrostatic potential $\varphi(z)$ was reduced to solving a modified Poisson–Boltzmann equation (only the case of 1:1 electrolyte is analyzed):

$$\frac{d^2\Phi}{dz^2} = \kappa^2 \sinh(\Phi)\exp\left(-\frac{u_v(z)}{k_BT}\right), \tag{3}$$

where $\Phi = e_0|\varphi|/k_BT$ is the positively defined dimensionless potential (k_BT is thermal energy, e_0 is unit charge),

$$\kappa = \left(8\pi e_0^2 C_t/\varepsilon k_BT\right)^{1/2} = \kappa_0 C_t^{1/2} \tag{4}$$

is the Debye screening parameter with ε being dielectric permittivity and C_t — total electrolyte concentration. The constant κ_0 is defined as $\kappa_0 = (8\pi e_0^2/\varepsilon k_BT)^{1/2}$. The integration of (Eq. (3)) gave (at $z=0$):

$$-\frac{1}{2\kappa\sinh(\Phi_0^S/2)}\left(\frac{d\Phi}{dz}\right)^S = \exp\left[-\frac{u_0}{2k_BT}(1-f_u)\right], \tag{5}$$

where f_u is a small correction, neglected hereafter (subscript "0" to the potential means that it refers to a system without specific adsorption of the counterions and the superscript "S" indicates value at $z=0$. To obtain (Eq. (5)), an iteration procedure was used consisting in replacing during the integration in the right hand side of (Eq. (3)) the exact dependence $\Phi(z)$ by the potential $\Phi_0(z)$ in the absence of specific effects. By coupling this result with the condition for electroneutrality of the system we arrived at a generalized form of the Gouy equation:

$$\Gamma = \frac{4\sqrt{C_t}}{\kappa_0}\sinh\frac{\Phi_0^S}{2}\exp\left(-\frac{u_0}{2k_BT}\right), \tag{6}$$

where Γ is surfactant adsorption. This equation was used to derive new version of Henry adsorption isotherm for ionic surfactants with specific effects:

$$\Gamma = KC^{2/3}; K = K_0\exp\left(-\frac{u_0}{2k_BT}\right); K_0 = \left(\frac{4K_s}{\kappa_0^2}\right)^{1/3}, \tag{7}$$

where K_s is the Henry adsorption constant of a neutral surfactant molecule with the same molecular structure as the surface active ion; K_0 is adsorption constant of the surface-active ion assuming zero value of the ion specific adsorption energy ($u_0=0$), K is adsorption constant of the surface-active ion accounting for the specific

adsorption energy and $C = C_s^{1/2}(C_s + C_{el})^{1/2}$ is the effective surfactant concentration [8] with C_s being surfactant concentration and C_{el} — concentration of added salt.

By comparing the equations for Henry law of adsorption of the ionized surfactant, expressed once by Φ^S and once — by Φ_0^S, and using (Eq. (6)) one arrives at the basic expression relating these potential to the ion adsorption energy u_0 [8]:

$$\Phi^S = \Phi_0^S + u_0 / 2k_BT. \tag{8}$$

If the surface potentials are presented in dimensional form, (Eq. (8)) becomes

$$\left|\varphi^S\right| = \left|\varphi_0^S\right| + u_0 / 2e_0. \tag{9}$$

The quantity $u_0/2e_0$ has dimension of electric potential and can be rightfully called *specific surface potential*. Because u_0 is negative (see Table 1), the field created by it will be opposite to that created by the surfactant layer and will decrease the latter. We will call φ^S *combined surface potential* because it is determined by both the purely electrostatic (φ_0^S) and the specific ($u_0/2e_0$) surface potentials. Eqs. (6) and (8) are the basic equations used below for the theoretical treatment of the experimental results on the critical micelle concentration, disjoining pressure of foam films and stability of emulsion drops.

2.2. Adsorption energy of the counterions

The adsorbed counterion displaces an ensemble of N_w water molecules filling the same volume V_i as the bare ion. Although each water molecule has its own energy, due to its interaction with the water molecules in the bulk phase, we will model this ensemble as a single large molecule, having the same geometry as the ion with which it interchanges positions. In Fig. 1A the positions of these molecules and the ion (1) before and (2) after ion adsorption are shown. Simple energy balance leads to

$$u_0 = u_{(2)} - u_{(1)} = \left(u_i^S + u_w^B\right) - \left(u_i^B + u_w^S\right) = \Delta u_i - \Delta u_w, \tag{10}$$

where subscripts "*i*" and "*w*" denote ion and water and superscripts "S" and "B"- surface and bulk state. If the hydration shell is not complete, the water molecules are pushed away by the interface, so that the bare ion of radius R_i can touch it (Fig. 1B) — exceptions are the ions Li^+, Na^+ and F^-, whose shells do not deform [8].

The energies in (Eq. (10)) were calculated by using the London expression (cf. e.g. [12]) for the intermolecular potential u_{kl} between molecules *k* and *l* at a distance r_{kl}:

$$u_{kl} = -\frac{L_{kl}}{r_{kl}^6}; L_{kl} = \frac{3}{2}\alpha_{0k}\alpha_{0l}\frac{I_k I_l}{I_k + I_l},$$

where L_{kl} is London constant with α_0 being static polarizability and *I* — ionization potential. The London potential was integrated over the volume of the water phase to calculate the energies corresponding to the four states in Fig. 1A. The result for the ion adsorption energy u_0 is:

$$u_0 = \frac{2}{3}\pi\rho_w\left(1 - \frac{3}{4}\frac{R_i}{R_h}\right)(L_{iw} - L_{ww}) \tag{11}$$

with

$$L_{iw} - L_{ww} = \frac{3}{2}\alpha_{0w}I_w\left(\frac{I_i}{I_i + I_w}\alpha_{0i} - \frac{N_w\alpha_{0w}}{2}\right). \tag{12}$$

In (Eq. (11)) ρ_w is the bulk particle number density of water and R_i and R_h are the radii of the bare and the hydrated ion respectively. When deriving (Eq. (12)) one has accounted for the fact that an ensemble of N_w water molecules must have polarizability $N_w\alpha_{0w}$. For ions with non-deformable shells one must set in (Eq. (11)) $R_i = R_h$. The hydrated ion radius R_h was calculated by using Marcus procedure [13], namely, from the equation

$$\frac{4\pi}{3}\left(R_h^3 - R_i^3\right) = n_w V_w \tag{13}$$

where the hydration number is $n_w = A_v|z_v|/R_i$, with z_v being ion valence and $A_v = 3.6$ Å for all ions. For radius of the water molecule we used $R_w = 1.38$ Å.

The specific ion adsorption energy u_0, defined by Eqs. (11) and (12), is the basic quantity we used in Ref. [8] and hereafter to characterize such different phenomena as surfactant adsorption, micellization, thin film disjoining pressure and emulsion drop coalescence. This single parameter encompasses the most important quantities, determining the occurrence of different ion specific phenomena: radii of the bare and hydrated ions, possible deformation of the hydration shell at the interface, polarizabilities and ionization

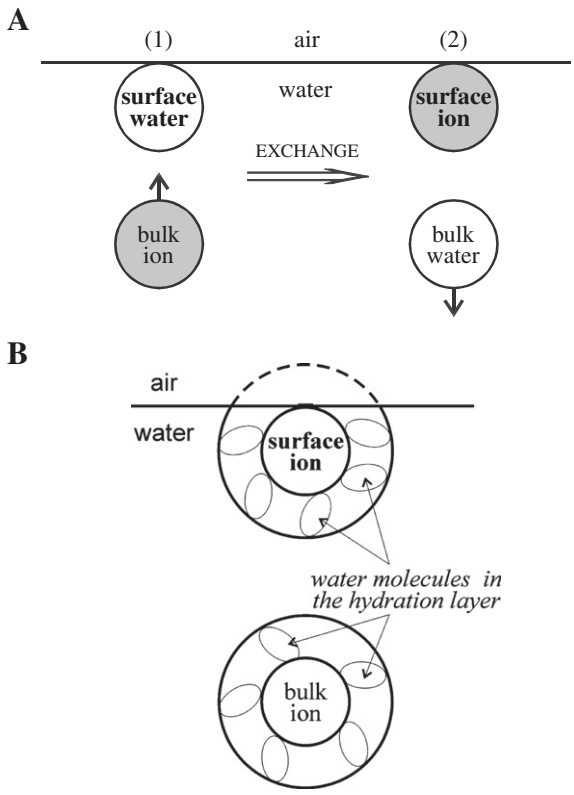

Fig. 1. Schematic presentation of the process of adsorption of an ion: A–(1) is ion in the bulk; A– (2) is ion at the interface; (B) – deformation of the hydration shell by the waiter/air interface. Figs. 7 and 8 from Ref. [8], with permission.

Table 1
Specific adsorption energies of some ions ($T = 25$ °C). Compare to the Hofmeister series, (Eq. (1)).

Cation:	Li^+	Na^+	NH_4^+	K^+	Rb^+	NMe_4^+
u_0/k_BT	−0.09	−0.34	−0.60	−0.97	−1.00	−1.03
Anion:	OH^-	F^-	Cl^-	Br^-	NO_3^-	N_3^-
u_0/k_BT	−0.16	−0.91	−1.49	−2.33	−2.87	−2.93

potentials of the ions and of the bulk phases (water and oil, if present). With Eqs. (11) and (12) and data for the quantities involved from Refs. [14,15], we calculated in Ref. [8] the values of u_0 for all ions considered. After the publication of Ref. [8], the above theory and procedure for calculation of u_0 were improved and new sources for the ion properties were used. The results were tested and confirmed against numerous experimental data for several surfactants and counterions (article in preparation). We quote in Table 1 these data for u_0/k_BT for the ions considered in the present article. Some of them are new, others are recalculated using slightly different parameters from those in Ref. [8].

3. Ion specific effects on CMC of ionic surfactants

3.1. Overview of the ion specific effects in micellar solutions

The self-assembly of ionic surfactants is an example where ion specific effects are of importance. The CMC of ionic surfactants sharing the same surface active ion and different counterions was investigated extensively experimentally [16,17]. Most of the data were found to obey "Hofmeister" series. Correlation to ion size and polarizability was also observed (see e. g. [9,10,18–20]). The CMC is not the only property of micellar solutions which depends on the nature of the counterion. Other properties, which show correlation to Hofmeister series include: the degree of binding (e.g. [21]); micelle aggregation number and shape [22,23]; clouding point [23]; enthalpy of micellization [24]; and viscosity of micellar solutions [25].

In this Section, the CMC of surfactant solutions will be explicitly related to the counterion adsorption energy, u_0. We confine ourselves to the case of ionic surfactants which are 1:1 electrolytes. We will account for the ion specific effects by generalizing the semi-empirical approach of Shinoda [16] which predicts CMC of ionic surfactants in the absence of Hofmeister effect. It is based on Gouy theory, and successfully explains the experimentally observed dependence of CMC on the electrolyte concentration C_{el}

$$\ln\ CMC = \text{const} - K_g\ \ln(CMC + C_{el}) \tag{14}$$

known as Corrin-Harkins equation [26,16,17].

3.2. Model

After Shinoda [16], we assume the micellar solution to consist of monomer solution (indexed with subscript "s") and micellar pseudo-phase (indexed with subscript "m"). The monomer solution of concentration C_s is assumed to be ideal, and the ionic surfactant to be totally dissociated. In such case, the chemical potential of the surfactant monomers will be

$$\mu_s = \mu_s^{\oplus} + k_BT\ \ln C_s; \tag{15}$$

here $\mu_s^{\oplus}$ is the standard chemical potential of the monomers. Following Shinoda, we assume also that the electrostatic contribution to the chemical potential is equal to the electrostatic work $E_{el} = K_g k_B T \Phi_0^S$ for transferring the surfactant (monovalent) ion into the micelle, i.e.

$$\mu_m = \mu_m^{\oplus} + K_g k_B T \Phi_0^S. \tag{16}$$

Here K_g is an empirical correction coefficient, whose physical meaning was discussed by Shinoda [16]. Shinoda conjectured that $0 < K_g < 1$ with the explanation that "it is logical to assume that every monomer introduces charge smaller than 1 into the micelle, due to the counterions that accompany it" [16]. Similar approach was used by other authors [27,28]. A more consistent approach would use Guntelberg charging process [29]. However, this approach is also questionable (cf. e.g. [30]); we preferred Shinoda approach because it has been verified by a large body of experimental data. The experimental K_g values typically lay in the range between 0.4 and 0.6, usually close to 1/2 [16].

The condition for chemical equilibrium is the equality of the potentials defined with Eqs. (15) and (16). If this equality is solved for the surfactant concentration C_s in the monomer solution, the following relation is obtained:

$$C_s = \exp\left(\frac{\mu_m^{\oplus} - \mu_s^{\oplus}}{k_BT}\right)\exp\left(K_g \Phi_0^S\right). \tag{17}$$

To determine C_s and Φ_0^S, we need also the electroneutrality condition, i.e. the Gouy equation. The curvature effect can be easily taken into account [29,31] but, following Shinoda, for the sake of simplicity we will neglect this effect. Hence, we will use the generalized Gouy equation for flat surface, (Eq. (6)). In the high potential approximation ($\Phi_0^S \gg 1$) and for monovalent ions one has

$$\exp\left(\Phi_0^S\right) = \frac{\kappa_0^2 \Gamma^2}{4C_t}\exp\left(\frac{u_0}{k_BT}\right). \tag{18}$$

Here Γ is the number of surfactant molecules per unit area of the micelle. Following Shinoda, we assume that Γ is independent of the salt concentration. Combining the equilibrium condition (17) with the Gouy Eq. (18), we obtain an equation for C_s:

$$C_s = \exp\left(\frac{\mu_m^{\oplus} - \mu_s^{\oplus}}{k_BT}\right)\left[\frac{\kappa_0^2}{4C_t}\Gamma^2 \exp\left(\frac{u_0}{k_BT}\right)\right]^{K_g}. \tag{19}$$

In the absence of added electrolyte, the ionic strength is equal to the surfactant concentration $C_t = C_s$, and (Eq. (19)) can be easily solved for C_s:

$$C_s^{1+K_g} = C_0^{1+K_g}\exp\left(\frac{K_g u_0}{k_BT}\right). \tag{20}$$

Here we introduced the standard CMC, C_0, defined with

$$C_0^{1+K_g} \equiv \exp\left(\frac{\mu_m^{\oplus} - \mu_s^{\oplus}}{k_BT}\right)\left(\frac{\kappa_0^2\Gamma^2}{4}\right)^{K_g} \tag{21}$$

C_0 is the CMC of the ionic surfactant in the absence of ion specific effects.

In the presence of 1:1 electrolyte, the total concentration is $C_t = C_s + C_{el}$, and we can then write (19) as follows:

$$C_s(C_s + C_{el})^{K_g} = C_0^{1+K_g}\exp\left(\frac{K_g u_0}{k_BT}\right). \tag{22}$$

In the absence of ion specific effects, one can set $u_0 = 0$, and (Eq. (22)) reduces to the classical Corrin–Harkins equation, (Eq. (14)), with the constant there replaced by $\ln C_0$:

$$\text{const} \equiv \ln C_0 = \frac{\mu_m^{\oplus} - \mu_s^{\oplus}}{k_BT(1+K_g)} + \frac{K_g}{1+K_g}\ln\frac{\kappa_0^2\Gamma^2}{4}. \tag{23}$$

Let us write Eqs. (20) and (22) in logarithmic form; in the absence of added electrolyte:

$$\ln C_s = \ln C_0 + \frac{K_g}{1+K_g}\frac{u_0}{k_BT}, \tag{24}$$

and in the presence of electrolyte:

$$lnC_s = \ln C_0 - \frac{K_g}{1+K_g}\left[-\frac{u_0}{k_BT} + \ln\left(1 + \frac{C_{el}}{C_s}\right)\right]. \tag{25}$$

(Eq. (25)) is a generalization of the Corrin–Harkins equation, (Eq. (14)): the undetermined constant in this equation is replaced by explicit expressions of a term, independent on the nature of the counterion (the standard CMC, C_0), and a term, independent on the nature of the surface active ion (the ion adsorption potential u_0).

3.3. Generalization to mixtures with two counterions

Eqs. (24) and (25) can be generalized for the important case where the ionic surfactant has one counterion, and the added electrolyte has another (this is the case of surfactant solution with salt additives). We will once again consider only the case where both electrolytes are 1:1. A more general form of Gouy equation for multicomponent counterions, including the specific interactions (i.e., u_{i0}) reads

$$\sum_i C_i\left[\exp\left(-\frac{e_i\varphi_0^S}{k_BT}\right)\exp\left(-\frac{u_{i0}}{k_BT}\right)-1\right]=\frac{\kappa_0^2}{4}\Gamma^2. \tag{26}$$

Here C_i is the concentration of the i-th counterion present in the solution, e_i is its absolute charge, u_{i0} is its adsorption potential. We will now use the high potential approximation ($\Phi_0^S \gg 1$). If only two monovalent counterions are present in the solution, (Eq. (26)) becomes:

$$\left[C_1\exp\left(-\frac{u_{10}}{k_BT}\right)+C_2\exp\left(-\frac{u_{20}}{k_BT}\right)\right]\exp\left(\Phi_0^S\right)=\frac{\kappa_0^2}{4}\Gamma^2. \tag{27}$$

This equation is analog of (Eq. (18)) for the case of two counterions (generalization for three and more counterions of different valence is straightforward). Commonly, one of the counterions is introduced into the solution with the ionic surfactant (so that $C_1 \equiv C_s$) and the other one is introduced with the added electrolyte ($C_2 \equiv C_{el}$). Expressing Φ_0^S from (Eq. (27)) and substituting it in the condition for chemical equilibrium (Eq. (17)), one obtains

$$C_s = C_0^{1+K_g}\left[C_s\exp(-u_{s0}/k_BT)+C_{el}\exp(-u_{el0}/k_BT)\right]^{-K_g} \tag{28}$$

where C_0 is defined by (Eq. (21)); u_{s0} is the adsorption energy of the counterion which came with the ionic surfactant, and u_{el0} is that of the counterion which came with the electrolyte added. The logarithmic form of (Eq. (28)) reads

$$\ln C_s = \left(1+K_g\right)\ln C_0 - K_g\ln\left[C_s\exp(-u_{s0}/k_BT)+C_{el}\exp(-u_{el0}/k_BT)\right]. \tag{29}$$

The relations Eqs. (28) and (29) are generalizations of Eqs. (22) and (25) (and resp. of the Corrin-Harkins equation, Eq. (14)) for the case of two different monovalent counterions. (Eq (29)) allows CMC of ionic surfactants (i.e. C_s) to be predicted at different salt concentrations and different counterions, if (**i**) the CMC of the surfactant in the absence of salt is known for one (standard) counterion (e.g. Na^+ for the anionic surfactants), and (**ii**) the adsorption energy of the counterion is known (see Table 1).

3.4. Comparison with experimental data

Experimental results for the ion specific effect on the CMC are summarized in the Supplementary material. From the whole set of data [9,10,16–19,23,32–57], only the data for 1:1 electrolytes were used. For solutions of surfactant with added salt, we used only the data with low electrolyte concentrations ($C_s + C_{el} < 15$ mM for all cationic surfactants, $C_s + C_{el} < 60$ mM for all anionic surfactants). The reason is that our model assumes **(i)** that the monomer solution is ideal, cf. (Eq. (15)), and **(ii)** that the surface potential of the micelle is high, cf. (Eq. (18)) — the second assumption fails with high electrolyte concentrations since the electrolyte lowers the surface potential. CMC values reported by different authors vary greatly, especially with the alkylsulfates. This forced us to carefully evaluate the data since they can vary by more than ±10% from source to source even if they are determined with the same method by different authors or with different methods by the same author. For this reason, in order to perform a convincing test of our model, we needed *many* measurements of CMC for surfactants with *many* different counterions and *many* salt concentrations.

Before proceeding further with the analysis of the experimental data let us check our computational procedure, which has an important problem: our equations in fact always contain two parameters of uncertain value — these are the constant K_g and the numerical coefficient before u_0/k_BT. The latter is theoretically 1 (cf. e.g. Eq. (25)) but can turn out to be different from this value when experimental data are processed. Let us assume for the moment that this coefficient has some undetermined value, K_u. Then (Eq. (25)) can be rewritten as:

$$\ln C_s = \ln C_0 - \frac{K_g}{1+K_g}\left[-K_u\frac{u_0}{k_BT}+\ln\left(1+\frac{C_{el}}{C_s}\right)\right]. \tag{30}$$

We will fit now by this equation some experimental data first by assuming that $K_g = 1/2$ and K_u is undetermined, and second — by assuming that $K_u = 1$ while K_g is undetermined. The data of Maiti et al. [9] for tetradecylammonium bromides ($C_{14}H_{29}NH_3Br$) were obtained by adding salts. The salt excess was not very large, but nonetheless (Eq. (25)) for single counterion turned out to be applicable. The results of the fit are presented in Fig. 2: (A) corresponds to assumed $K_u = 1$ and gave $K_g = 0.45$, and (B) corresponds to assumed $K_g = 1/2$ and gave $K_u = 0.90$. The small deviation of the obtained results from $K_u = 1$ and $K_g = 1/2$ entitles us to use the latter values in all further calculations. This conclusion is confirmed also by the results in Figs. 6 and 8.

The theory is checked with experimental data for alkyltrimethylammonium salts (Figs. 3–6) and dodecylsulfate salts (Figs. 7–9). The data for CMC of the homologous series of alkyltrimethylammonium salts, ($C_{10}H_{21} \div C_{18}H_{37}$)$NMe_3^+$ ("Me" denotes methyl group), in the absence of added salts [16,17,19,34–43,46,47,50–52,56] are presented in Fig. 3. They were obtained with data from 62 measurements with 17 different surfactants. According to (Eq. (24)) they are plotted as ln C_s vs. $-u_0/k_BT$. The CMC follows the Hofmeister series, (cf. Eq. (1)). The linear dependence, following from (Eq. (24)) is obeyed, within the experimental accuracy. The slope is fixed to 1/3, corresponding to $K_g = 1/2$. The intercept is the only fitting parameter, and gives the standard CMC, C_0. The values of C_0 depend on the structure of the surface active ion, but not on the counterion, cf. (Eq. (21)). The C_0 values, determined from Fig. 3, are presented in Fig. 4, as function of the carbon chain length, n. They follow the known linear dependence $\ln C_0 = A + B\,n$ where the value of the slope B coincides with the known value $B = -\ln 2$, valid for all monovalent non-branched ionic surfactant [16,58]. The value of the intercept, obtained as fitting parameter, namely $A = 11.9$, refers to the whole alkyltrimethylammonium salts homologous series. The above values of A and B along with knowledge of the counterion adsorption energy u_0 (see Table 1 for list of u_0 values) allow predicting the CMC of any alkyltrimethylammonium salt.

The data from Fig. 3 are plotted in Fig. 5 as C_s/C_0 vs. $-u_0/k_BT$. All data fall on the same curve — indeed, according to (Eq. (24)) the ratio C_s/C_0 depends only on u_0/k_BT. The effect of the counterion is quite large — its change can shift CMC by about ±50%.

Similar results were obtained for alkylpyridinium ion, $C_nH_{2n+1}Pyr^+$, with Cl^- and Br^- as counterions. The respective experimental data [16,17,32,50,57] are not so rich as those for $C_nH_{2n+1}NMe_3^+$. Still, the CMC data for $n = 12$, 14 and 16 and counterions Cl^- and Br^- could be interpreted in the same way as it was done with the alkyltrimethylammonium salts in Fig. 3. For saving space the respective figure is given in the Supplementary material.

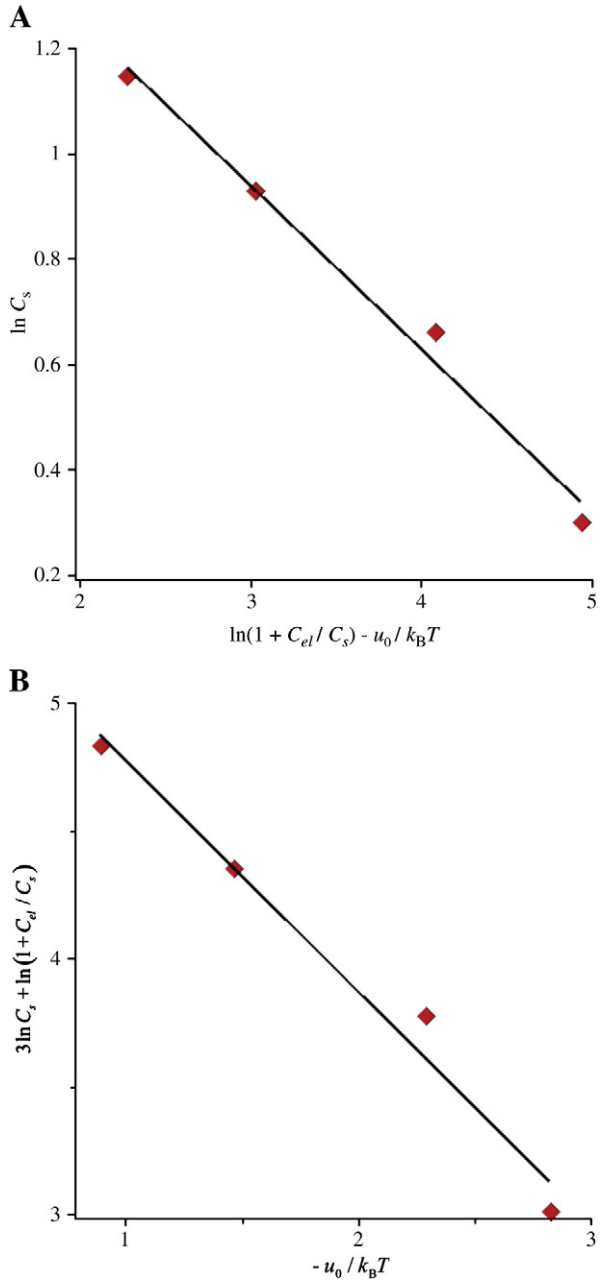

Fig. 2. Plot of the data from Ref. [9] for tetradecyltrimethylammonium bromide ($C_{14}H_{29}NMe_3Br$) with added salt NaX ($X^- = F^-$, Cl^-, Br^-, NO_3^-) according to (Eq. (30)). (A) ln C_s vs. $\ln(1 + C_{el}/C_s) - u_0/k_BT$ is plotted assuming that $K_u = 1$. The slope of this dependence is −0.31, corresponding to $K_g = 0.45$, close to the expected value 1/2. (B) $[(1 + K_g)/K_g]\ln C_s + \ln(1 + C_{el}/C_s)$ vs. $-u_0/k_BT$ is plotted assuming that $K_g = 1/2$. The slope of this dependence is −0.90, corresponding to $K_u = 0.9$ which is close to its theoretical value $K_u = 1$.

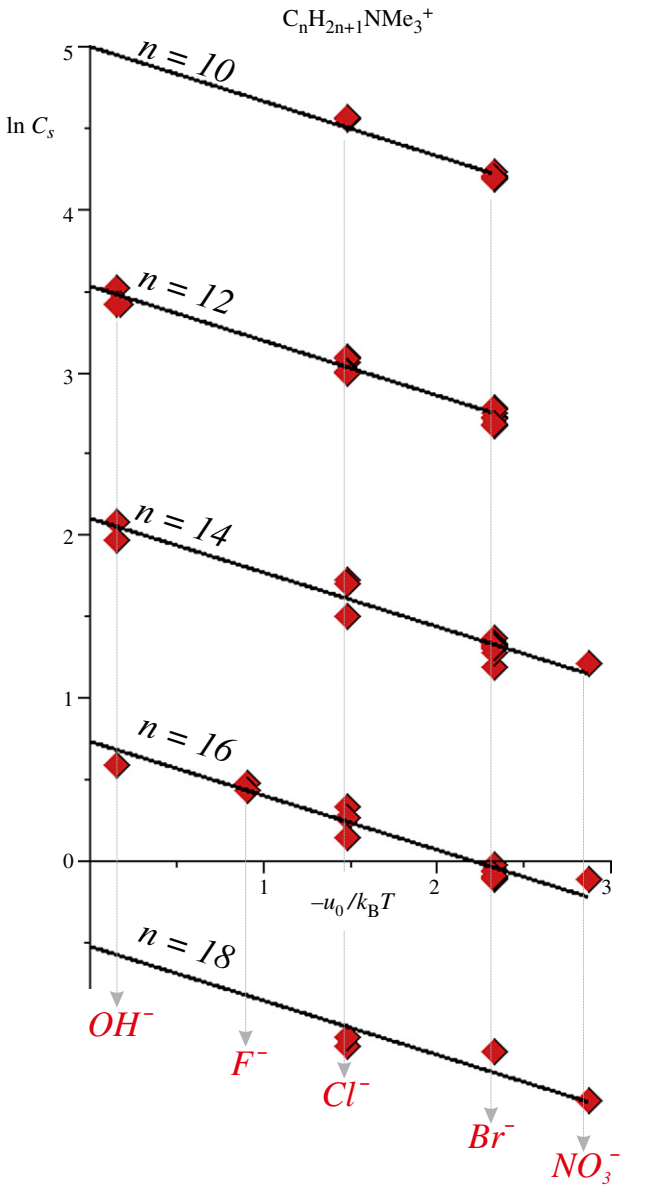

Fig. 3. Dependence of ln C_s [mM] on the counterion adsorption energy $-u_0/k_BT$ for different carbon chain lengths n of the surface active alkyltrimethylammonium ion $C_nH_{2n+1}NMe_3^+$ [19,16,17,34–43,46,47,50–52,56]; $T = 25 \div 30$ °C. The black parallel lines are the theoretical dependences according to (Eq. (24)) with $K_g = 1/2$. The slope is consequently $K_g / (1 + K_g) = 1/3$ for all lines. The values of ln C_0, obtained from the intercepts, depend on n (see Fig. 4 below). The source data are given in the Supplementary material.

The data for CMC of $C_{14}H_{29}NMe_3^+$ in the presence of mixture of counterions are presented in Fig. 6. Typically, the Br^- counterion came with the surfactant, and the second counterion was added with the salt (source data can be found in the supplementary material). The concentration of both ions was commensurable. The data are fitted well by our (Eq. (29)) with slope $K_g = 1/2$.

The CMC of $C_{12}H_{25}SO_4^-$ salts with no salt added [9,10] at $T = 30 \div 33$ °C are shown in Fig. 7. In contrast to the adsorption energies of most common *anions*, u_0 for most common *cations* do not differ much. Indeed, the difference in $-u_{i0}/k_BT$ between K^+ and Li^+ is 0.85, whereas between Br^- and F^- it is 1.39 – see Table 1. This complicates the test of the model. Still, (Eq. (24)) with $K_g = 1/2$ compares well with the data. A better test of the theory is possible with the data of Goddard [18] for CMC of $C_{12}H_{25}SO_4Na$ in the presence of added salts (Li_2SO_4, Na_2SO_4, K_2SO_4, NMe_4I). They are plotted in Fig. 8, along with data from other authors [10,24,49] — all points fall on a line drawn according to (Eq. (29)) with slope $K_g = 1/2$.

The test of our model with dodecylammonium $C_{12}H_{25}NH_3^+$ and dodecanoates $C_{12}H_{25}COO^-$ salts with various counterions [16,17] was less successful. The data followed the linear dependence of ln C_s on u_0/k_BT, as required by (Eq. (24)), but the value of K_g was significantly smaller than $K_g = 1/2$. We suppose that this is due to possible hydrolysis of the surface active ion.

Most authors work by using a surfactant with one ion (e.g. Na^+ for $C_{12}H_{25}SO_4Na$) and salt with another, and not always the counterion added with the salt is in large excess. Then, a legitimate question arises: is (Eq. (25)) still valid at small values of the concentration ratio added counterion vs. basic counterion? To answer this question, we

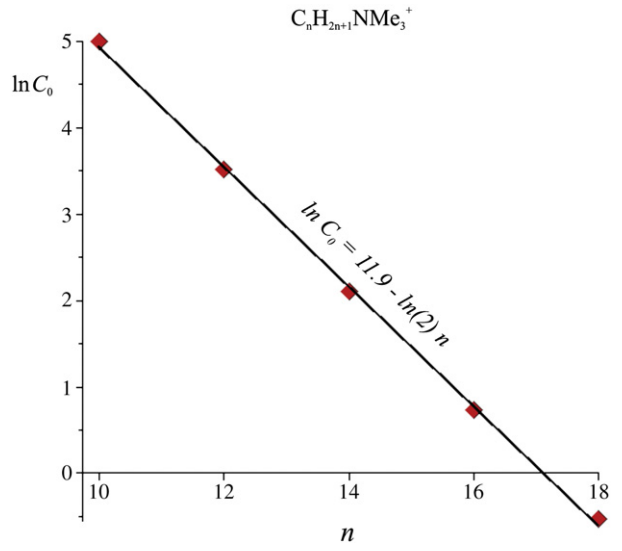

Fig. 4. Dependence of ln C_0 [mM] on the carbon chain length n of the surface active ion $C_nH_{2n+1}NMe_3^+$. The values of C_0 were obtained from the intercept of the CMC dependence on the adsorption energy, ln $C_s(u_0)$, shown in Fig. 3. The value of the slope of the linear dependence ln $C_0 = A + B{\cdot}n$ is $B = -\ln 2$ [16,58].

notice that (Eq. (29)) can be reduced to (Eq. (25)) by setting $u_{s0} = u_{el0}$ in $\ln[C_s \exp(-u_{s0}/k_BT) + C_{el} \exp(-u_{el0}/k_BT)]$. This is equivalent to consider a mixture of one basic ion, say Na^+, and an added ion, say K^+, as a single component K^+. We will try to analyze this problem by using the data of Goddard [18] (see also Fig. 9) at small concentration of the added counterion. His initial point for $C_{12}H_{25}SO_4Na$ with added NMe_4^+ corresponds to ratio NMe_4^+:$Na^+ = 0.19$; similarly, with added K^+, the initial point is at K^+:$Na^+ = 0.66$. We have plotted the data for small salt concentration in Fig. 9A according to (Eq. (25)), and in Fig. 9B — according to (Eq. (29)). The slopes in Fig. 9A are $K_g = 0.61$ and 0.77 for K^+ and NMe_4^+ respectively. The same data, plotted in Fig. 9B, exhibit the same value, $K_g = 1/2$, both for K^+ and NMe_4^+, with some small difference of the intercepts, probably due to ion specific

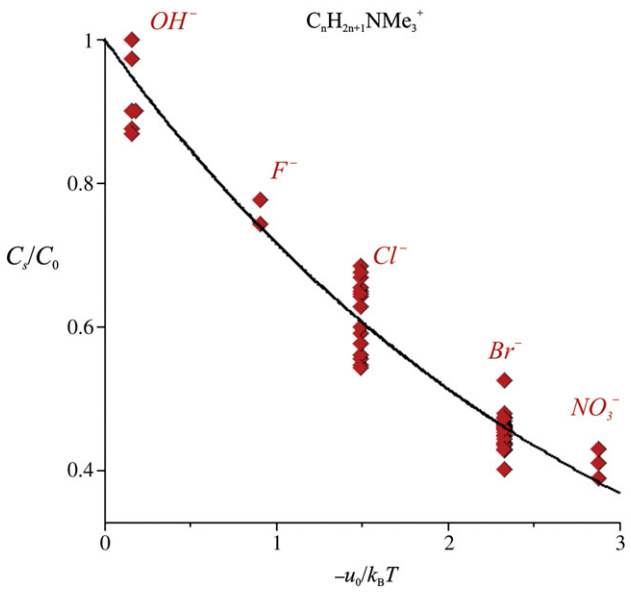

Fig. 5. Normalized CMC, C_s/C_0, vs. the counterion adsorption energy $-u_0/k_BT$ for alkyltrimethylammonium, $C_nH_{2n+1}NMe_3^+$ (n = 10÷18), salts with different anions. In agreement with (Eq. (24)), the normalized CMC does not depend on the carbon chain length n – that is why all experimental points from Fig. 3 fall now on a single curve. For a given chain length n, the type of the counterion of the surface active ion $C_nH_{2n+1}NMe_3^+$ can shift the CMC more than 2 times.

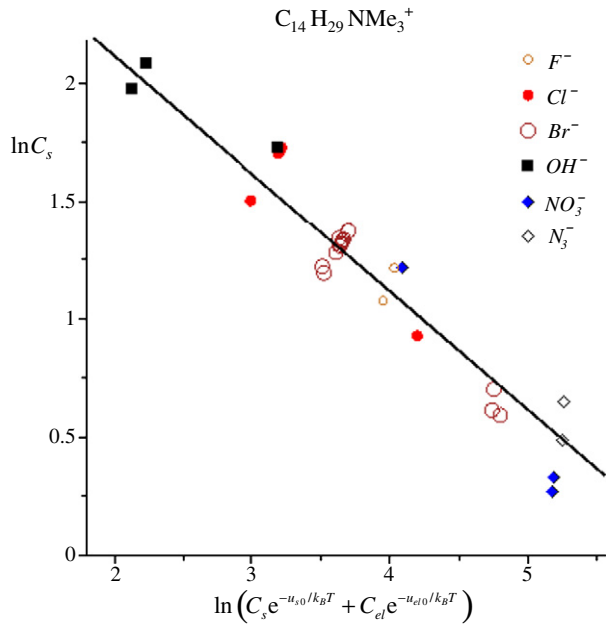

Fig. 6. Dependence of ln C_s on the added salt concentration and the ions adsorption energy u_0, according to (Eq. (29)). The points are experimental data for tetradecyltrimethylammonium ion $C_{14}H_{29}NMe_3^+$ with different anions and anion mixtures, with and without added salt. The symbol "F^-" refers to $C_{14}H_{29}NMe_3Br$ with added NaF [9]; "Cl^-" – to $C_{14}H_{29}NMe_3Cl$ alone [17,35,38,39,44], or $C_{14}H_{29}NMe_3Br$ with added NaCl [9]; "Br^-" – to $C_{14}H_{29}NMe_3Br$ alone [34,38,40,46], or $C_{14}H_{29}NMe_3Br$ with added bromides [9,34]; "OH^-" – to $C_{14}H_{29}NMe_3OH$ alone [43,46]; "NO_3^-" – to $C_{14}H_{29}NMe_3NO_3$ alone [42], or $C_{14}H_{29}NMe_3Br$ with $NaNO_3$ [9]; "N_3^-" – to $C_{14}H_{29}NMe_3Br$ with added NaN_3 [9]. The line is the theoretical dependence, (Eq. (29)), with slope $K_g = 1/2$. $T = 25 \div 30$ °C. Source data can be found in the Supplementary material.

effect on the value of Γ, which affects the standard CMC value C_0 in (Eq. (29)). The significant difference of the slopes in Fig. 9A from the value $K_g = 1/2$ suggests that to obtain reliable results for such small values of the counterion ratio, one must use the more sophisticated (Eq. (29)).

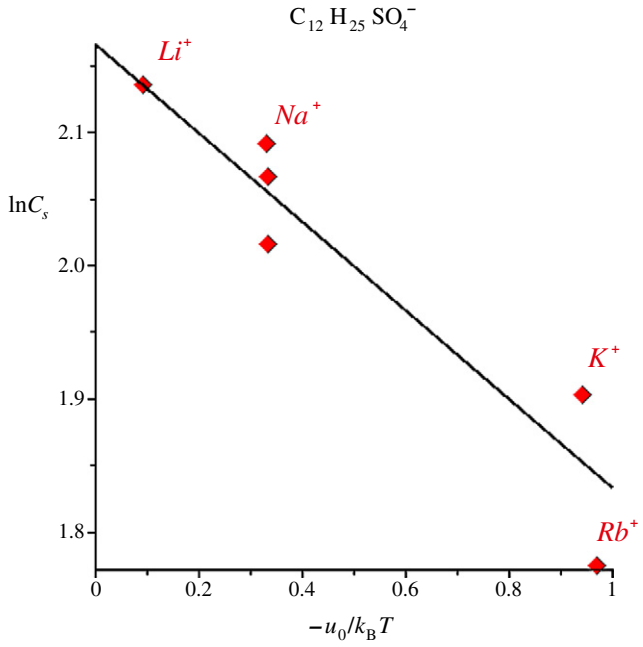

Fig. 7. ln C_s vs. ion adsorption energy $-u_0/k_BT$ for dodecylsulfate anion $C_{12}H_{25}SO_4^-$ salts with different counterions [9,10]. The black line is drawn according to (Eq. (24)) with $K_g = 1/2$, so that the slope is fixed to 1/3. $T = 30 \div 33$ °C. Source data can be found in the Supplementary material.

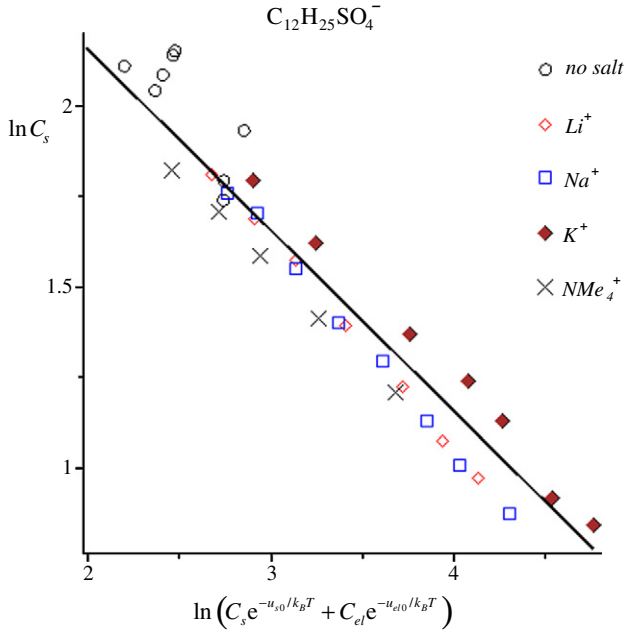

Fig. 8. Dependence of ln C_s on the added salt concentration and the ions adsorption energy u_0, according to (Eq. (29)). The empty circles are data for dodecylsulfate, $C_{12}H_{25}SO_4^-$, with counterions Li^+, Na^+, K^+, Rb^+ and NMe_4^+ (without added salt) [18,10,23,49]; "Li^+" denotes data for $C_{12}H_{25}SO_4Na$ with added Li^+ salts [18]; "Na^+" denotes $C_{12}H_{25}SO_4Na$ with added Na^+ salts [18]; "K^+" denotes $C_{12}H_{25}SO_4Na$ with added K^+ salts; "NMe_4^+" denotes $C_{12}H_{25}SO_4Na$ with added NMe_4^+ salts [18]. The line is the theoretical dependence according to (Eq. (29)), with slope $K_g = 1/2$; $T = 40$ °C. See the Supplementary material for the source data.

4. Thin liquid films

4.1. Materials and method

We measured the disjoining pressure of aqueous films in air (foam films) stabilized by 1 mM solutions of hexadecyltrimethylammonium bromide ($C_{16}H_{33}NMe_3Br$ > 99%, Sigma). Similar films separate the bubbles in a foam (or the drops in an emulsion) and play a major role for its stability. In order to study the ion specific effect the experiments were carried out by adding to the studied solutions excess amounts (9 mM) of one of the following salts: NaF, NaCl or NaBr (Merck, analytical grade) — it was shown in Ref. [8] that such excess amount of a given counterion is sufficient to make it dominant in the diffuse electric layer. The aqueous solutions were prepared with deionized water, purified by a Milli-Q system (Millipore). The experiments were carried out at the natural pH without additional adjustment, at room temperature, 25 °C.

The disjoining pressure, stabilizing the films, was measured in a thin film pressure balance by using the Mysels-Jones porous plate technique (see Fig. 10) [59,60]. The film was formed from a biconcave droplet in a hole of 1 mm diameter, drilled into a porous glass disk. The disjoining pressure isotherms were obtained by measuring interferometrically the film thickness after applying a fixed pressure, measured by pressure transducer PX26-005DV, Omega Engineering Inc. (accuracy ± 20 Pa). The film thickness, h, was calculated from the measured intensity, I, of the reflected monochromatic light [61]:

$$h = \lambda / 2\pi n_r \left(l\pi \pm \arcsin\sqrt{\frac{I - I_{min}}{I_{max} - I_{min}}} \right) \quad (31)$$

where I_{max} and I_{min} denote the maximal and minimal intensity of the reflected light; $l = 0, 1, 2, \ldots$ is order of interference, λ is wavelength of the used monochromatic light (546 nm in our case), and n_r is refractive index of the liquid forming the film (water).

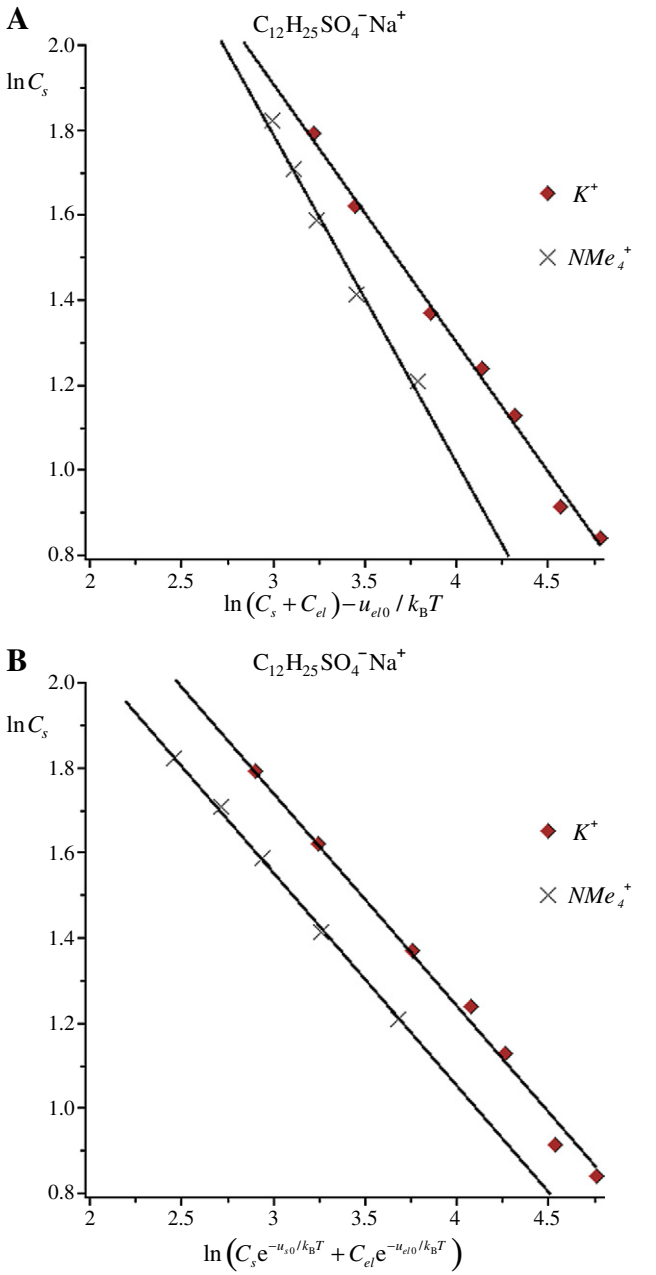

Fig. 9. Comparison of the ln C_s dependence on the added salt concentration and the ions adsorption energy u_0, treated by means of the two-component (Eq. (29)) and by means of the one-component generalized Corrin–Harkins (Eq. (25)). Fig. 9A. Plot of the data of CMC of sodium dodecylsulfate, $C_{12}H_{25}SO_4Na$, in the presence of K^+ or NMe_4^+ counterions from Ref. [18] according to (Eq. (25)), plotted as ln C_s vs. $\ln(C_s + C_{el}) - u_{el0}/k_BT$, see the text for details. The lines are linear fits with slopes $K_g = 0.61$ and 0.77 for the K^+ and NMe_4^+ counterions correspondingly. Fig. 9B. Plot of the same data according to (Eq. (29)) as ln C_s vs. $\ln[C_s \exp(-u_{s0}/k_BT) + C_{el} \exp(-u_{el0}/k_BT)]$. The lines are plots of (Eq. (29)) with slope $K_g = 1/2$.

4.2. Results and discussion

The theory of the electrostatic disjoining pressure has been developed by many authors, above all by Derjaguin and associates. Their results are summarized in the excellent book of Churaev et al. [62]. According to their theory (neglecting the ion specific effects) the electrostatic disjoining pressure, Π_{el}, in a planar film of low surface potential or large thickness is given by the following expression:

$$\Pi_{el} = 64 k_B T C_t \tanh^2\left(\Phi_0^S / 4\right) \exp(-\kappa h) = \Pi_0 \exp(-\kappa h) \quad (32)$$

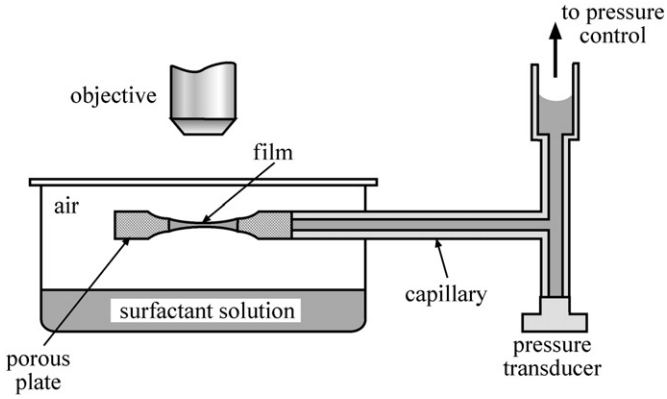

Fig. 10. Schematic presentation of the porous plate cell.

where C_t is total ion concentration. Since during the derivation of (Eq. (32)) in [62] no other assumptions about the surface potential were done, we decided that in order to account for the specific effects it should be sufficient merely to replace Φ_0^S with Φ^S by means of (Eq. (8)).

(Eq. (32)) suggests that the dependence of the experimental disjoining pressure Π on the thickness h should be close to linear in coordinates ln Π vs. h. Fig. 11 shows that indeed this is the case. Since the films are rather thick, one can disregard the contribution of the van der Waals disjoining pressure (direct numerical calculations confirmed this). This permits identifying Π with Π_{el} and using (Eq. (32)) for the calculation of Π, but with Φ^S replacing Φ_0^S. The lines in Fig. 11 are almost parallel and obey the equation

$$\ln \Pi_{el} = \ln \Pi_0 - \kappa h. \tag{33}$$

The obtained intercepts lnΠ_0 and slopes κ are shown in Table 2.

The almost parallel, but shifted, lines suggest that the specific ion interactions (if any) are affecting mostly the surface potential Φ^S. By means of (Eq. (32)) we calculated the experimental values of Φ^S from the obtained data for Π_0 (see Table 2) and plotted in Fig. 12 the results as Φ^S vs. $-u_0/k_BT$. The relatively good linearity and close value of the experimental slope, 0.4, to the theoretical one, 1/2, (cf. Eq. (8)) seem to confirm the role of the ion specific effect.

The Hofmeister effect on the surface potential and the disjoining pressure, Π, is by no means negligible. To appreciate it for films closer to reality, in Fig. 13 we present the results (obtained in Ref. [8]) for the total disjoining pressure Π_{total} (including also the van der Waals contribution with Hamaker constant $A_H = 4\times10^{-20}$ J) of foam films with 0.5 mM of the halide counterions. The maxima of $\Pi(h)$ around $h = 5$ nm control the stability and the coalescence of the bubbles. The maximum is more than 4 times lower in the presence of only 0.5 mM

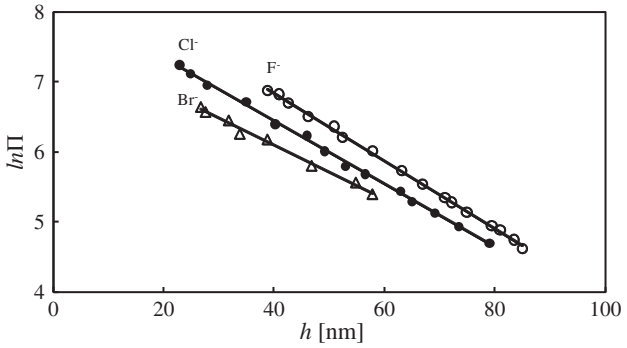

Fig. 11. Plot of ln Π vs. h for foam films stabilized with $C_{16}H_{33}NMe_3Br$ and NaX (X = F⁻, Cl⁻, Br⁻).

Table 2
Intercepts, ln Π_0, and slopes, κ, of the lines in Fig. 11.

Ion	F⁻	Cl⁻	Br⁻
lnΠ_0 [Pa]	8.79	8.25	7.65
κ [nm^{-1}]	0.0485	0.0451	0.0386

Br than it would have been with the same electrolyte concentration if the ion specific effects were disregarded.

5. Emulsion stability

5.1. Materials

We performed measurements of the emulsion stability with two types of techniques — Film Trapping Technique (FTT) and Centrifugation. We used the same surfactant ($C_{16}H_{33}NMe_3Br$), salts (NaF, NaCl or NaBr), water and temperature as in Section 4. The concentrations of the surfactant and the added salts for FTT were the same as in the thin film studies (Section 4), but for the centrifugation the emulsions with 1 mM salts were too unstable, so that the concentrations of the added salts were increased to 30 mM. Soybean oil, purified by passing it through a glass column filled with Silicagel 60 adsorbent, was used as oil phase.

5.2. Film trapping technique

The film trapping technique (FTT), developed in Refs. [63–65] is a useful method for determining the coalescence stability of single emulsion drops. The principle of the FTT is the following: A vertical capillary, partially filled with oil, is held at a small distance above the flat bottom of a glass vessel, Fig. 14. The lower edge of the capillary is immersed in the working solution, which contains dispersed micronsize oil drops. The capillary is connected to a pressure control system, which allows one to vary and to measure precisely the difference, ΔP_A, between the air pressure in the capillary, P_A, and the atmospheric pressure, P_A^0. The pressure is measured by a pressure transducer PX26-005DV, Omega Engineering Inc. (accuracy ± 20 Pa), connected to a personal computer. Upon the increase of P_A the oil–water meniscus in the capillary moves downward against the substrate. When the distance between the oil–water meniscus and the glass substrate becomes smaller than the drop diameter, some of the drops remain entrapped in the formed glass–water–oil layer. The pressure P_A is increased until the coalescence of the entrapped oil drops with the upper oil phase is observed. The capillary pressure in the moment of drop coalescence, P_C^{CR}, represents the coalescence

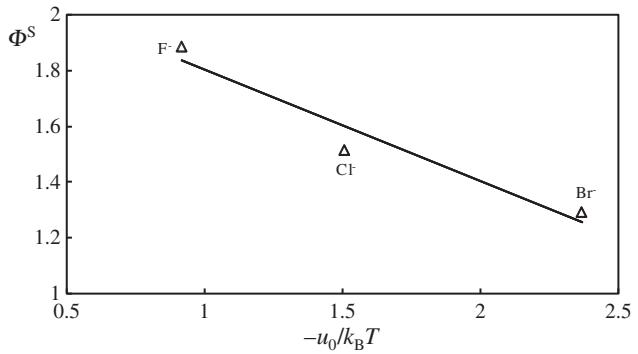

Fig. 12. Combined surface potential Φ^S vs. $-u_0/k_BT$ for foam films stabilized with $C_{16}H_{33}NMe_3Br + NaX$ (X = F⁻, Cl⁻, Br⁻). The slope is −0.4. The potential Φ^S was determined from the line intercepts in Fig. 11 and (Eq. (33)); the values of u_0 are listed in Table 2. The intercept yelds the purely electrostatic potential, $\Phi_0^S = 2.2$. The absolute value of the slope is 0.4 (compare to the theoretical value 1/2 in Eq. (8)).

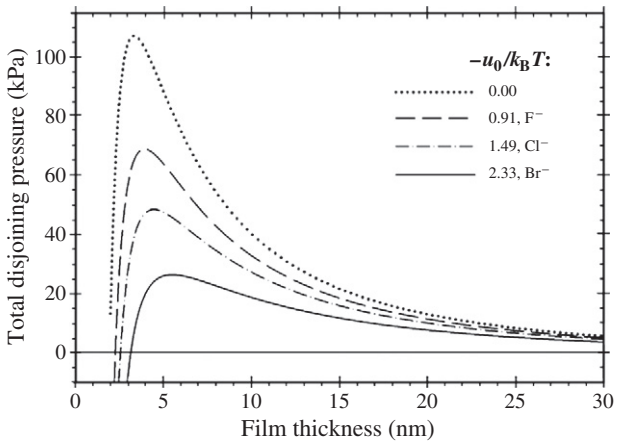

Fig. 13. Total disjoining pressure Π_{total} calculated with Hamaker constant $A_H = 4\times10^{-20}$ J for 0.5 mM counterions F^-, Cl^- and Br^- (from Ref. [8], with permission).

barrier and is called *critical capillary pressure*. It is related to ΔP_A in the moment of drop breakage and can be calculated from the equation:

$$P_C^{CR} = \Delta P_A - \Delta P_{OIL} - \rho g z, \tag{34}$$

where ΔP_{OIL} is the pressure jump across the oil column in the capillary. It includes contributions from the hydrostatic pressure of the oil column and the capillary pressure of the air/oil meniscus. It is measured after filling the FTT capillary with oil but before immersing the capillary into the water pool. In the hydrostatic term z is the depth of the water (see Fig. 14), ρ is the water mass density and g is gravity acceleration. The trapped oil drops and the coalescence process were observed from above with an optical microscope (Jenavert, Carl Zeiss Jena, Germany). A description of the technical details and theoretical considerations can be found in Ref. [66].

5.3. Centrifugation

The procedure is basically the same as in Ref. [67]. Oil-in water emulsions were prepared by stirring for 4 min a mixture of 40 mL water phase and 10 mL soybean oil (20 vol. % SBO) with a rotor-stator homogenizer, Ultra Turrax T25 (Janke & Kunkel GmbH & Co, IKA-Labortechnik), operating at 13 500 rpm. The drop size d_{32} was determined by optical microscopy of specimens of the studied

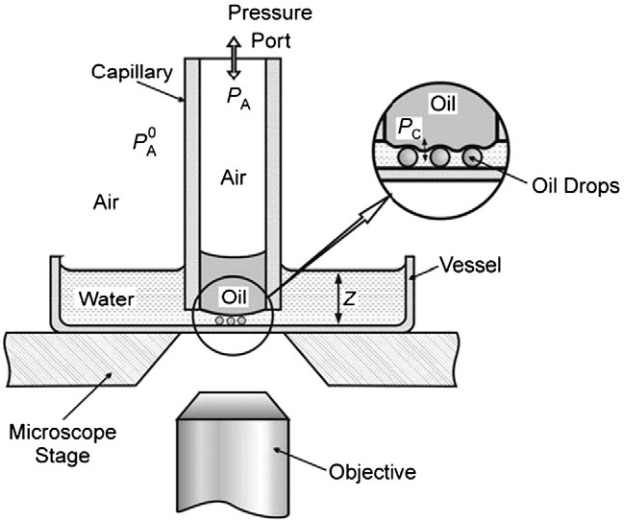

Fig. 14. Scheme of the film trapping apparatus and of the droplets trapped between the oil-water and the substrate (see the magnification lens), from Ref. [66] with permission.

emulsions in transmitted light with microscope Axioplan (Zeiss, Germany), equipped with objective Epiplan, ×50, and connected to a CCD camera (Sony) and VCR (Samsung SV-4000). After 30 min storage the fresh emulsions were transferred into several centrifugal tubes and centrifuged at 25 °C in 3 K15 centrifuge (Sigma Laborzentrifugen, Germany). The emulsion stability is characterized by the critical osmotic pressure, P_{OSM}^{CR}, at which a continuous oil layer is released at the top of the emulsion cream in the centrifuge tube. P_{OSM}^{CR} is calculated from the experimental data by using the equation :

$$P_{OSM}^{CR} = \Delta\rho g_k \left(V^{OIL} - V^{REL}\right) / A = \Delta\rho g_k \left(H^{OIL} - H^{REL}\right) \tag{35}$$

where $\Delta\rho$ is the difference between the mass densities of the aqueous and the oil phases; g_k is the centrifugal acceleration ($g_k = L\omega^2$, where L is the distance between the axis of rotation and the center of the cream, ω is the angular velocity); V_{OIL} is the *total volume of oil* used for preparation of the emulsion; V_{REL} is the volume of *released oil* at the end of centrifugation; and A is the cross-sectional area of the centrifuge test tube.

5.4. Results and discussion

The system parameters and the measured values of the critical pressures P_C^{CR} and P_C^{CR} are tabulated in Table 3 and plotted in Fig. 15 as P_C^{CR} (solid line) and P_{OSM}^{CR} (dashed line) vs. $-u_0/k_BT$. These critical pressures are proportional to Π and the higher their values are, the more stable the emulsions.

We do not dispose of enough information to carry out the same detailed analysis of these phenomena as we did with the electrostatic disjoining pressure. For example, we have no idea what the film thickness is; it is not quite clear whether a planar film forms or how much the disjoining pressure is affected by the curvature of the very small drops-these effects make problematic the calculation of the electrostatic disjoining pressure by means of (Eq. (32). Still, some qualitative conclusions are possible. The linear dependence of P_C^{CR} and P_{OSM}^{CR} on $-u_0/k_BT$ confirms the presence of specific effects. However, instead of decreasing with the increase of $-u_0/k_BT$ (as the electrostatic disjoining pressure does) the critical pressures are increasing. Therefore, the electrostatic disjoining pressure Π_{el} is not the repulsive pressure to be overcome in order for the coalescence to occur. But then, what is the reason for the ion specific effect, demonstrated in Fig. 15? It is not possible to answer with certitude this question without detailed studies of the phenomena accompanying the coalescence process. Nevertheless we dare suggesting a hypothesis. The role of the specific effect of the counterions is twofold. On one side, it decreases the height of the maxima of the disjoining pressure (see Fig. 13) thus making easier for the thin film to avoid the electrostatic repulsive pressure and to thin to thinner (metastable) Newton black film, where another, short range repulsive disjoining pressure (most probably steric or osmotic) might be operative. It must be overcome for the thin film to rupture. On the other side, no matter what the nature of this disjoining pressure is, it must increase with the surfactant adsorption, Γ. However, unlike the electrostatic disjoining

Table 3
Critical pressures and drop sizes of SBO-in-water emulsions, stabilized with 1 mM $C_{16}H_{33}NMe_3Br$ with added NaF, NaCl and NaBr.

C_t [mM]	C_s [mM]	C_{el} [mM]	Electrolyte	d_{32} [μm]	FTT, P_C^{CR} [Pa]	Centrifuge, P_{OSM}^{CR} [Pa]
10	1	9	NaF	25.2	360	–
10	1	9	NaCl	28.5	1100	–
10	1	9	NaBr	27.0	1320	–
31	1	30	NaF	20.7	–	360
31	1	30	NaCl	22.4	–	640
31	1	30	NaBr	21.5	–	917

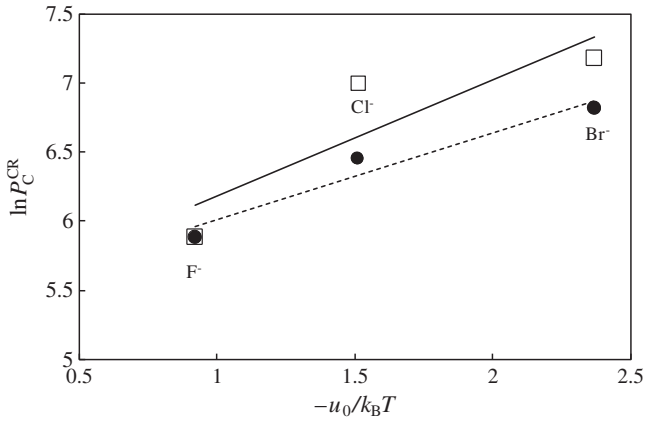

Fig. 15. Critical pressures P_C^{CR} (by FTT, solid line) and P_{OSM}^{CR} (by centrifugation, dashed line) vs. $-u_0/k_BT$ of oil-in-water emulsions stabilized by $C_{16}H_{33}NMe_3Br + NaX$ (X = F⁻, Cl⁻, Br⁻). (□)P_C^{CR} of oil-in-water emulsion films stabilized by 10^{-3} M $C_{16}H_{33}NMe_3Br + 9\times10^{-3}$ M NaX (X = F⁻, Cl⁻, Br⁻) obtained by FTT (slope = 0.85); (•) P_{OSM}^{CR} of oil-in-water emulsion films stabilized by 10^{-3} M $C_{16}H_{33}NMe_3Br + 3\times10^{-2}$ M NaX (X = F⁻, Cl⁻, Br⁻) obtained by centrifuge (slope = 0.63).

pressure, the surfactant adsorption, Γ, increases (for a given bulk surfactant concentration) with $-u_0/k_BT$ (cf. Eq. (7)). This brings us to the second role of the ion specific effects — it is to increase the short range repulsive pressure created by the surfactant, thus stabilizing the thin film. This explains why the slopes of the lines in Fig. 15 are positive. They should have been negative if only the electrostatic disjoining pressure Π_{el} were stabilizing the film. To support this opinion in Fig. 16 we have plotted the maxima of Π_{total} from Fig. 13 (which are in fact the coalescence barriers) vs. $-u_0/k_BT$ –indeed, the slope is negative. This means that the short range repulsive pressure involved in the stability of the emulsion drops is not directly related to ion specific effects. The theoretical and experimental verification of this hypothesis is feasible but it is time consuming and beyond the scope of this paper.

6. Conclusion

Our main goal in this study was to apply our approach from Ref. [8] quantifying theoretically the Hofmeister effect by introducing the ion specific adsorption energy u_0, to the analysis of three phenomena: (**i**). Micellization (CMC); (**ii**). Thin film disjoining pressure (Π); and (**iii**). Critical pressure for coalescence of emulsion drops (P^{CR}). The essence of our approach was to use existing theories of CMC [16] and Π [62] by replacing the non-specific surface potential Φ_0^S with the combined surface potential $\Phi^S = \Phi_0^S + u_0/2k_BT$ or, by using the generalized Gouy (Eq. (6)), including the specific effect.

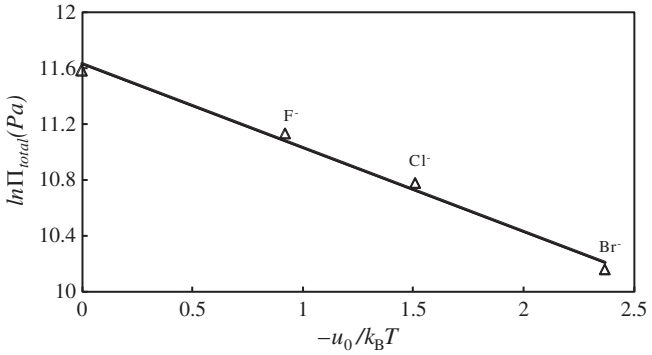

Fig. 16. Total disjoining pressure Π_{total} in the maxima in Fig. 13 vs. $-u_0/k_BT$. This is in fact the coalescence barrier according to DLVO theory.

The modification we did on Shinoda's model [16] allowed us to explain successfully the experimental observations of ion specific effects on CMC found by many authors [16,17,19,34–43,46,47,50–52,56]. We used our approach for three cases of practical importance: (**i**) CMC of a given surface active ion with various counterions without added salt, (Eq. (24)); (**ii**) CMC of a given surface active ion in the presence of added salt with the same counterion as the surfactant, (Eq. (25)); and (**iii**) CMC of ionic surfactant with one (basic) counterion in the presence of added salt with another counterion, (Eq. (29)). Our theoretical results compared well (within the experimental error) with the CMC data for a number of ionic surfactants without and with different added salts.

We measured the disjoining pressure Π vs. the thickness h of thin liquid films, stabilized by $C_{16}H_{33}NMe_3Br$ with excess amounts of counterions F⁻, Cl⁻ and Br⁻. From the intercepts, ln Π_0, of the linear plots of ln Π vs. the film thickness h (Fig. 11) we calculated the surface potentials Φ^S and plotted them in Fig. 12 against $-u_0/k_BT$. The relatively good linearity of the plot and its slope, 0.4, which is close to the theoretical one, 1/2, are consistent with our theory. The total disjoining pressure, Π_{total}, revealed very strong specific effect, leading to its considerable decrease – for example, its maximum for counterion Br⁻ is four times lower than in the absence of specific effects (see Fig. 13).

The critical coalescence pressure, P_C^{CR}, of single emulsion drops, stabilized by $C_{16}H_{33}NMe_3Br$ with excess amounts of counterions F⁻, Cl⁻ and Br⁻ was determined by the Film Trapping Technique (FTT). The analogous pressure, P_{OSM}^{CR}, for drops in an emulsion was determined by centrifugation. The plots of ln P_C^{CR} and ln P_{OSM}^{CR} vs. $-u_0/k_BT$ (see Fig. 15) gave a surprising result — they were linear but *increasing* with $-u_0/k_BT$. We hypothesized that this is due to the lowering of the coalescence barrier and the rise of the surfactant adsorption, both due to the ion specific effect — this should lead to the appearance of a short range repulsive disjoining pressure, which increases with $-u_0/k_BT$.

The obtained results on CMC, electrostatic disjoining pressure and emulsion drops stability not only follow the Hofmeister series for the phenomena studied, but also give its quantitative characterization. It is worthwhile noting that no adjustable fitting parameter was used in the computational procedure for u_0. Moreover, the straight lines on almost all figures, referring to the critical micelle concentration (viz. Figs. 2,3,6,7,8 and 9B), were drawn with fixed value of the parameter $K_g = 1/2$ (or $K_u = 1$ in Fig. 2B) and the only free parameter was the intercept, which is not related to the interpretation of the ion specific effect. All this should make our results reliable. We believe that the counterion specific adsorption energy, u_0, introduced in Ref. [8] and used also here, encompasses all major factors, controlling the Hofmeister effect on the studied phenomena (cf. Section 2.2). If this is confirmed by analysis of more phenomena, revealing Hofmeister effect, one could claim that u_0 is the "ONE factor involved in Hofmeister effects" [4].

Acknowledgment

This work was supported by National Science Fund Grants DVU 02/54 and DVU 02/12.

Appendix A. Supplementary data

Supplementary data to this article can be found online at doi:10.1016/j.cis.2011.06.002.

References

[1] Hofmeister F. About regularities in the protein precipitating effects of salts and the relation of these effects with the physiological behaviour of salts. Archiv fuer experimentelle Pathologie und Pharmakologie 1887;XXIV:247–60.

[2] Heydweiller A. Concerning the physical characteristics of solutions in correlation. II. Surface tension and electronic conductivity of watery salt solutions. Annalen Der Physik 1910;33:145–85.
[3] Curr Opin Colloid Interface Sci 2004;9.
[4] Kunz W, Lo Nostro P, Ninham BW. The present state of affairs with Hofmeister effects. Curr Opin Colloid Interface Sci 2004;9:1–18.
[5] Ninham BW, Yaminsky V. Ion binding and ion specificity: the Hofmeister effect and Onsager and Lifshitz theories. Langmuir 1997;13:2097–108.
[6] Bostroem M, Williams DRM, Ninham BW. Surface tension of electrolytes: specific ion effects explained by dispersion forces. Langmuir 2001;17:4475–8.
[7] Bostrom M, Williams DRM, Ninham BW. Specific ion effects: why DLVO theory fails for biology and colloid systems. Phys Rev Lett 2001;87 168103/1-/4.
[8] Ivanov IB, Marinova KG, Danov KD, Dimitrova D, Ananthapadmanabhan KP, Lips A. Role of the counterions on the adsorption of ionic surfactants. Adv Colloid Interface Sci 2007;134–135:105–24.
[9] Maiti K, Mitra D, Guha S, Moulik SP. Salt effect on self-aggregation of sodium dodecylsulfate (SDS) and tetradecyltrimethylammonium bromide (TTAB): physicochemical correlation and assessment in the light of Hofmeister (lyotropic) effect. J Mol Liq 2009;146:44–51.
[10] Lu JR, Marrocco A, Su T, Thomas RK, Penfold J. Adsorption of dodecyl sulfate surfactants with monovalent metal counterions at the air–water interface studied by neutron reflection and surface tension. J Colloid Interface Sci 1993;158:303–16.
[11] Bostroem M, Williams DRM, Ninham BW. Ion specificity of micelles explained by ionic dispersion forces. Langmuir 2002;18:6010–4.
[12] Israelachvili JN. Intermolecular and surface forces. New York: Acad. Press; 1985.
[13] Marcus Y. Thermodynamics of ion hydration and its interpretation in terms of a common model. Pure Appl Chem 1987;59:1093–101.
[14] Marcus Y. Ion properties. New York: Marcel Dekker, Inc.; 1997.
[15] CRS Handbook of Chemistry and Physics, Internet version. http://www.hbcpnetbase.com/2006.
[16] Shinoda K, Nakagawa T, Tamamushi B-I, Isemuta T. Colloidal surfactants, some physicochemical properties. New York and London: Academic Press; 1963.
[17] Rosen MJ. Surfactants and interfacial phenomena. Third ed. New York: Wiley; 2004.
[18] Goddard ED, Harva O, Jones TG. The effect of univalent cations on the critical micelle concentration of sodium dodecyl sulfate. Trans Faraday Soc 1953;49:980–4.
[19] Jakubowska A. Interactions of different counterions with cationic and anionic surfactants. J Colloid Interface Sci 2010;346:398–404.
[20] Jiang N, Li PX, Wang YL, Wang JB, Yan HK, Thomas RK. Aggregation behavior of hexadecyltrimethylammonium surfactants with various counterions in aqueous solution. J Colloid Interface Sci 2005;286:755–60.
[21] Gaillon L, Lelievre J, Gaboriaud R. Counterion effects in aqueous solutions of cationic surfactants: electromotive force measurements and thermodynamic model. J Colloid Interface Sci 1999;213:287–97.
[22] Joshi JV, Aswal VK, Bahadur P, Goyal PS. Role of counterion of the surfactant molecule on the micellar structure in aqueous solution. Curr Sci 2002;83:47–9.
[23] Benrraou M, Bales BL, Zana R. Effect of the nature of the counterion on the properties of anionic surfactants. 1. Cmc, ionization degree at the cmc and aggregation number of micelles of sodium, cesium, tetramethylammonium, tetraethylammonium, tetrapropylammonium, and tetrabutylammonium dodecyl sulfates. J Phys Chem B 2003;107:13432–40.
[24] Ropers MH, Czichocki G, Brezesinski G. Counterion effect on the thermodynamics of micellization of alkyl sulfates. J Phys Chem B 2003;107:5281–8.
[25] Kumar S, Sharma D, Kabir-ud-Din. Effect of additives on the clouding behavior of sodium dodecyl sulfate plus tetra-n-butylammonium bromide system. J Surfactants Deterg 2004;7:271–5.
[26] Corrin ML, Harkins WD. The effect of salts on the critical concentration for the formation of micelles in colloidal electrolytes. JACS 1947;69:683–8.
[27] Nagarajan R. Micellization, mixed micellization and solubilization — the role of interfacial interactions. Adv Colloid Inreface Sci 1986;26:205–64.
[28] Rao IV, Ruckenstein E. Micellization behavior in the presence of alcohols. J Colloid Interface Sci 1986;113:375–87.
[29] Srinivasan V, Blankschtein D. Effect of counterion binding on micellar solution behavior: 1. Molecular-thermodynamic theory of micellization of ionic surfactants. Langmuir 2003;19:9932–45.
[30] Spitzer JJ. Maxwellian double layer forces: from infinity to contact. Langmuir 2003;19:7099–111.
[31] Evans DF, Mitchell DJ, Ninham BW. Ion binding and dressed micelles. J Phys Chem 1984;88:6344–8.
[32] Rosen MJ, Dahanayake M, Cohen AW. Relationship of structure to properties in surfactants .11. Surface and thermodynamic properties of N-dodecylpyridinium bromide and chloride. Colloids Surf 1982;5:159–72.
[33] Brady JE, Evans DF, Warr GG, Grieser F, Ninham BW. Counterion specificity as the determinant of surfactant aggregation. J Phys Chem 1986;90:1853–9.
[34] Zielinski R. Micelle formation in aqueous NaBr solutions of alkyltrimethylammonium bromides. Pol J Chem 1998;72:127–36.
[35] Malliaris A, Lang J, Zana R. Micellar aggregation numbers at high surfactant concentration. J Colloid Interface Sci 1986;110:237–42.
[36] Bales BL, Zana R. Characterization of micelles of quaternary ammonium surfactants, as reaction media I: Dodeclytrimethylammonium bromide and chloride. J Phys Chem B 2002;106:1926–39.
[37] Para G, Jarek E, Warszynski P. The Hofmeister series effect in adsorption of cationic surfactants — theoretical description and experimental results. Adv Colloid Inreface Sci 2006;122:39–55.
[38] Perger TM, Bester-Rogac M. Thermodynamics of micelle formation of alkyltrimethylammonium chlorides from high performance electric conductivity measurements. J Colloid Interface Sci 2007;313:288–95.
[39] Durand-Vidal S, Jardat M, Dahirel V, Bernard O, Perrigaud K, Turq P. Determining the radius and the apparent charge of a micelle from electrical conductivity measurements by using a transport theory: explicit equations for practical use. J Phys Chem B 2006;110:15542–7.
[40] Evans DF, Wightman PJ. Micelle formation above 100-degrees-C. J Colloid Interface Sci 1982;86:515–24.
[41] Grieger PF, Kraus CA. Properties of electrolytic solutions .35. Conductance of some long chain salts in methanol–water mixtures. JACS 1948;70:3803–11.
[42] Gonzalez-Perez A, Czapkiewicz J, Del Castillo JL, Rodriguez JR. Micellar properties of tetradecyltrimethylammonium nitrate in aqueous solutions at various temperatures and in water-benzyl alcohol mixtures at 25 degrees C. Coll Polym Sci 2004;282:1359–64.
[43] Hashimoto S, Thomas JK, Evans DF, Mukherjee S, Ninham BW. Unusual behavior of hydroxide surfactants. J Colloid Interface Sci 1983;95:594–6.
[44] Hayami Y, Ichikawa H, Someya A, Aratono M, Motomura K. Thermodynamic study on the adsorption and micelle formation of long chain alkyltrimethylammonium chlorides. Coll Polym Sci 1998;276:595–600.
[45] Larsen JW, Magid LJ. Calorimetric and counterion binding studies of interactions between micelles and ions — observation of lyotropic series. JACS 1974;96:5774–82.
[46] Lianos P, Zana R. Use of pyrene excimer formation to study the effect of Nacl on the structure of sodium dodecyl-sulfate micelles. J Phys Chem 1980;84:3339–41.
[47] Mehta SK, Bhasin KK, Chauhan R, Dham S. Effect of temperature on critical micelle concentration and thermodynamic behavior of dodecyldimethylethylammonium bromide and dodecyltrimethylammonium chloride in aqueous media. Coll Surf A 2005;255:153–7.
[48] Paredes S, Tribout M, Sepulveda L. Enthalpies of micellization of quaternary tetradecyltrimethylammonium and cetyltrimethylammonium. J Phys Chem 1984;88:1871–5.
[49] Flockhart B. Effect of temperature on critical micelle concentration of some paraffin-chain salts. J Coll Sci 1961;16:484.
[50] Klevens HB. Critical micelle concentrations as determined by refraction. J Phys Coll Chem 1948;52:130–48.
[51] Osugi J, Sato M, Ifuku N. Micelle formation of cationic detergent solution at high pressures. Rev Phys Chem Jpn 1965;35:32.
[52] Okuda H, Imae T, Ikeda S. The adsorption of cetyltrimethylammonium bromide on aqueous surfaces of sodium–bromide solutions. Colloids Surf 1987;27:187–200.
[53] Johnson SB, Drummond CJ, Scales PJ, Nishimura S. Electrical double-layer properties of hexadecyltrimethylammonium chloride surfaces in aqueous-solution. Colloid Surf A 1995;103:195–206.
[54] Meguro K, Kondo T, Ohba N, Ino T, Yoda O. A new analytical method of electroconductivity data of surfactant solutions.1. Bull Chem Soc Jpn 1957;30:760–5.
[55] Meguro K, Kondo T, Ohba N. A new analytical method of electroconductivity data of surfactant solutions.3. Bull Chem Soc Jpn 1958;31:472–6.
[56] Brady AP, Ross S. The measurement of foam stability. J Am Chem Soc 1944;66:1348–56.
[57] Ford WPJ, Ottewill RH, Parreira HC. Light-scattering studies on dodecylpyridinium halides. J Colloid Interface Sci 1966;21:522.
[58] Scott AB, Tartar HV, Lingafelter EC. Electrolytic properties of aqueous solutions of octyltrimethylammonium octanesulfonate and decyltrimethylammonium decanesulfonate. JACS 1943;65:698–701.
[59] Mysels KJ, Jones MN. Direct measurement of variation of double-layer repulsion with distance. Discuss Faraday Soc 1966:42–50.
[60] Bergeron V, Radke CJ. Equilibrium measurements of oscillatory disjoining pressures in aqueous foam films. Langmuir 1992;8:3020–6.
[61] Scheludko A. Thin liquid films. Adv Colloid Interface Sci 1967;1:391–464.
[62] Churaev NV, Derjagiun BV, Muller VM. Surface forces. Springer; 1987.
[63] Ivanov IB, Hadjiiski A, Denkov ND, Gurkov TD, Kralchevsky PA, Koyasu S. Energy of adhesion of human T cells to adsorption layers of monoclonal antibodies measured by a film trapping technique. Biophys J 1998;75:545–56.
[64] Hadjiiski A, Dimova R, Denkov ND, Ivanov IB, Borwankar R. Film trapping technique — precise method for three-phase contact angle determination of solid and fluid particles of micrometer size. Langmuir 1996;12:6665–75.
[65] Hadjiiski A, Tcholakova S, Ivanov IB, Gurkov TD, Leonard EF. Gentle film trapping technique with application to drop entry measurements. Langmuir 2002;18:127–38.
[66] Tcholakova S, Denkov ND, Ivanov IB, Campbell B. Coalescence in beta-lactoglobulin-stabilized emulsions: effects of protein adsorption and drop size. Langmuir 2002;18:8960–71.
[67] Tcholakova S, Denkov ND, Sidzhakova D, Ivanov IB, Campbell B. Effects of electrolyte concentration and pH on the coalescence stability of beta-lactoglobulin emulsions: experiment and interpretation. Langmuir 2005;21:4842–55.